



CHORUS

This is the accepted manuscript made available via CHORUS. The article has been published as:

Scaling and spatial analysis of the dielectric response of cadmium selenide nanowires

Yosuke Kanai and Giancarlo Cicero

Phys. Rev. B **90**, 165417 — Published 14 October 2014

DOI: [10.1103/PhysRevB.90.165417](https://doi.org/10.1103/PhysRevB.90.165417)

Scaling and Spatial Analysis of Dielectric Response of Cadmium Selenide Nanowires

Yosuke Kanai*

Department of Chemistry
University of North Carolina, Chapel Hill, NC, USA

Condensed Matter and Materials Division
Lawrence Livermore National Laboratory, CA, USA

Giancarlo Cicero

Department of Applied Science and Technology
Politecnico of Torino, Italy

ABSTRACT

Transverse dielectric response of hexagonal cadmium selenide (CdSe) nanowires was investigated using first principles quantum mechanical calculations. Scaling behavior of polarizability was found to closely follow a simple dielectric cylinder model even for small nanowires with a diameter of a few nanometers. The spatial dependence of the dielectric response in the nanowires was analyzed in terms of maximally localized Wannier functions in order to elucidate the model behavior. Localized d-electrons at cadmium atoms were found responsible for the simple analytic scaling of the polarizability, and the dielectric response in the center of nanowire was found converged to that of bulk already for 3 nm diameter nanowires.

* To whom correspondence should be addressed
ykanai@unc.edu

I. INTRODUCTION

Developing a quantitative understanding of how optical and electronic properties of materials change with its size is of paramount importance for a wide range of technological applications¹. In particular, dielectric properties of semiconductor materials have been studied extensively, and how the dielectric response changes with the size for nano-materials is becoming increasingly important not only for designing technological devices² but also for assembling nano-materials using external electric fields³. For instance, dielectrophoresis has been used to align various nanowires in experiments⁴. At a fundamental level, it is of interest to understand how the dielectric response changes spatially inside a material as its dimension reduces to nano-scale limit in nano-particles and nanowires^{1, 5, 6}. As these materials become smaller in size, the surface-to-volume ratio increases dramatically, and the spatial dependence of the dielectric response is expected to be highly non-uniform.

Cadmium selenide (CdSe) nano-materials are of great interest particularly because they are widely synthesized experimentally and also used for various technological applications ranging from solar cell^{7, 8} to biological imaging⁹. We have theoretically investigated the dielectric response of small hexagonal CdSe nanowires (NWs) using a generalization of the local analysis proposed by Wu, et al¹⁰. Using the real-space analysis based on representation in maximally localized Wannier functions^{11, 12}, we provide spatial analysis of the dielectric response in the NWs. We employed first-principles electronic structure calculations based on density functional theory (DFT) to investigate how the electronic polarizability (or equivalently static dielectric constant at microscopic scale) scales for small CdSe nanowires. Our results show that this quantity converges fast with increasing nanowire size and that the core of the nanowire already behaves as bulk CdSe even for a small diameter of ~ 2 nm.

II. THEORETICAL METHOD

DFT calculations¹³ are performed with the generalized gradient approximation of Perdew-Burke-Ernzerhof (PBE)¹⁴ for the exchange and correlation potential. Ultrasoft pseudopotentials were used to describe the valence-core interactions of electrons¹⁵, including scalar relativistic effects of the core electrons. Wavefunctions and charge densities were expanded in plane waves with kinetic energies up to 27 and 200 Rydberg, respectively. Periodic boundary conditions and Monkhorst-Pack k-point sampling with a (811) grid are used in Brillouin zone integration. External electric fields are applied in the nanowire transverse direction using a saw-tooth finite-field. The approach by Kozinsky and Marzari was used to remove the depolarization field stemming from the periodic boundary conditions⁵. Electronic-enthalpy method¹⁶ was used to apply the electric field for bulk CdSe. Maximally Localized Wannier Functions (MLWF) are obtained by performing a unitary transformation on the occupied Kohn-Sham single-particle orbitals using WANN program¹⁷.

III. RESULTS AND DISCUSSION

We investigated CdSe NWs in wurtzite (hexagonal) form with a range of diameter in 0.5~3 nm as shown in Figure 1 and Table 1. The geometries of all the NWs were fully optimized with the all residual forces being less than 10^{-5} a.u.. The energy gaps for the NWs are likely to be underestimated due to the use of the semi-local exchange-correlation functional in DFT as discussed for bulk CdSe in comparison to GW calculations by Yang, et al.¹⁸. The NWs have hexagonal cross-section, possessing non-polar (1 $\bar{1}$ 00) facets, and they are periodic along the wire axis. Unlike the case of ZnO¹⁹, we did not observe a significant change in the lattice constant along the NW axis (i.e. 7.13 Å for NWs compared to 7.12 Å of the bulk CdSe value) except for the smallest NW which has a lattice constant of 6.91 Å (Table 1). At the atomistic level, the surface Cd-Se dimers buckle slightly by $\sim 5^\circ$, resulting in increased charge transfer at

surface. Figure 2 shows the extent of the charge transfer change in a Cd-Se pair at (1 $\bar{1}$ 00) surface of bulk CdSe as a function of the surface depth. Electron charge displacement is enhanced significantly for the top surface, and this is expected to play an important role for nano-materials as the surface-to-volume ratio becomes large.

We begin by discussing what a simple analytical model of electrostatics would predict for the transverse polarizability (per unit length) of NWs. The transverse polarizability (α_{\perp}) of a NW can be estimated using a dielectric cylinder model

$$\alpha_{\perp} = \frac{1}{2} \frac{\epsilon - 1}{\epsilon + 1} R^2$$

where R is the cylinder radius and ϵ is the bulk dielectric constant. Our calculated transverse dielectric constant (high-frequency limit) for bulk CdSe is 6.97, which is close to the value of 7.2 obtained previously by Mohr and Thomsen using DFT-LDA²⁰ while the experimental value is 6.3²¹. For the atomistic hexagonal NWs we investigated here, we take the largest distance measured in terms of atomic positions as the radius R in the dielectric cylinder model. The NW polarizabilities obtained from first-principles calculations for the structures reported in Figure 1 are compared to the values predicted by this model using both the calculated and experimental dielectric constants of bulk CdSe (see Figure 3). For all the NW diameters studied here, this simple model underestimates the polarizability, but the relative error becomes expectedly smaller with the increasing diameter. At the same time, the underestimation is only around 40 % even for the smallest NW. Given the simplicity of the electrostatic model, this order-of-the-magnitude agreement is quite impressive and the agreement is likely to be better for larger NWs, for which first-principles calculations would be prohibitively expensive in terms of computational resources. Importantly, we found that the scaling behavior of the transverse polarizability from the first-principles calculations shows a linear dependence on the radius squared as in the dielectric cylinder model. Such behavior is not intuitive because of the very high surface-to-volume ratio at this small scale and the significant charge transfer at the surfaces of CdSe NWs.

In order to obtain insights into this observation, we now discuss how the spatial dependence of the polarizability can be analyzed. We propose here a theoretical approach to quantify the electronic polarizability of anisotropic systems such as nanowires at microscopic level. In terms of spatially-localized maximally Localized Wannier functions (MLWF), “polarizability“ of individual MLWFs can be examined as they linearly contribute to the overall polarizability of single NWs. According to the modern theory of polarization²², the macroscopic polarization of a crystal can be defined with respect to a reference system (P_{ref}) and can be written in terms of MLWFs as

$$\Delta P = P - P_{ref} = \frac{1}{\Omega} (e \sum_l Z_l \Delta R_l - 2e \sum_i \Delta r_i^W)$$

where Ω is the volume of the unit cell, r_i^W are the positions of the individual Wannier centers, and R_l are the ionic positions. For a periodic system, ΔP is defined modulo $2e\mathbf{R}_l/\Omega$, with \mathbf{R}_l being the lattice vector along the periodic direction. Expressing the polarization in terms of localized MLWF, Cicero and co-workers¹⁹ investigated how the spatially-dependent “*local dipole*” varies in wurtzite ZnO nanowires. Building upon this approach, one could investigate spatially-dependent *local polarizability* in the following way. Macroscopic dielectric constant (ϵ) is formally related to polarizability (α), and it can be expressed in terms of MLWFs, as

$$\begin{aligned} \epsilon &= 1 + \frac{4\pi}{\Omega} \alpha = 1 + \frac{4\pi}{\Omega} \sum_i \alpha_i \\ &= 1 + \frac{4\pi}{\Omega} \sum_i \frac{1}{E} (r_i^{W,E} - r_i^{W,0}) \end{aligned}$$

where $r_i^{W,0}$ and $r_i^{W,E}$ are the Wannier centers in the unperturbed system and under applied electric field (E) in the linear regime, respectively. We can then define the individuals α_i as “local polarizability”, which provides a convenient framework for discussing the spatially-dependent dielectric response of materials as done analogously in Ref.¹⁹ for polarization. The concept of *local polarizability* is widely employed (although not uniquely defined) in molecular systems²³ (for example in constructing model potential for classical molecular dynamics), and MLWF transformation provides a natural avenue for partitioning the overall polarizability. In the present case of nanowires, we are concerned with polarizability per unit length.

In order to understand the simple analytical scaling behavior observed for the polarizability change with the NW diameter, we analyze how each MLWF polarizes individually. We define here density of Wannier states (DOWS) as a function of the local polarizability per unit length as

$$D(\alpha) = \int d\alpha' \sum_i^{Occ} |\langle w_i(r; \alpha') | w_i(r; \alpha) \rangle|^2 \delta(\alpha - \alpha')$$

where $w_i(r; \alpha')$ are the MLWFs with the local polarizability α' , which is well defined in the linear response regime for individual MLWFs. The calculated $D(\alpha)$ are shown in Fig. 4 for all NWs, averaged between the two transverse directions along which the electric field is applied, namely the $[1\bar{1}00]$ and $[11\bar{2}0]$ directions. It is apparent that there is dominant contribution from those MLWF with local polarizability less than 0.1 a.u.. The significant peak originates from the completely filled 4d-shell of the cadmium atoms, which do not participate in forming chemical bonding with selenium atoms. Although each d-electron does not contribute appreciably to the overall polarizability of the individual NWs because of their small local polarizability, the large numbers of the Cd d-electrons make the overall contribution substantial. Indeed, the reason that the overall NW polarizability scales as an idealized dielectric cylinder model is that its dominant contribution comes from these d-electrons whose local polarizability depends only weakly on the local structures and thus weakly on the NW diameter.

In the DOWS (Fig. 4), a well-defined double-peaked feature appears in the range 0.3~0.5 a.u. with increasing NW diameter. This mainly derives from polarized Cd-Se chemical bonds (see Fig. 5). To further analyze the spatial dependence of the polarizability, the DOWS is spatially decomposed in terms of different concentric hexagonal shells for each studied NW and also as a function of the applied electric field direction, namely the $[1\bar{1}00]$ and $[11\bar{2}0]$ directions. The results are reported in Figure 6. Generally, the features in the DOWS are more defined for larger NWs and for the shells that are closer to the center of the NWs. In the largest NW-IV (~3 nm), the DOWS for the inner most shell (first shell) is visually identical to that of bulk CdSe (after normalizing it by the number of electrons). The dielectric response in the first shell is essentially converged to the bulk behavior even for NW-III (~2 nm). However, the DOWS are still quite different in the first shell for NW-I and NW-II. In both NW-IV and NW-III, the second shell shows also similar DOWS as for the first shell, but not in smaller NWs.

For the largest nanowire (NW-IV), we considered also the effect of molecular passivation at the surface due to surfactants present during solution-based synthesis of NWs. Trioctylphosphine oxides often passivate the surface of CdSe nano-materials in experiments^{24, 25}. Recent work shows that surface ligands can significantly modify the surface polarization of CdSe nano-materials²⁶. Instead of typical trioctylphosphine oxides with long alkane chains, for computational convenience, we considered here trimethylphosphine oxide molecules as surfactant at 50% coverage as shown in Fig. 7. CdSe-NW surface rearrangement and polarizability change are expected to depend mainly on the phosphine anchoring group rather than on the chain length of the attached alkyl groups. The overall DOWS profile does not show appreciable change for the CdSe NW itself (excluding the contributions from surfactant molecules). However, analyzing the dielectric response in terms of individual shell contributions and by the applied field direction reveals that the surfactant molecules introduce a significant local field effect in large local polarizability ranges as shown in Fig. 8. Except for the dominant d-electron peak with the local

polarizability less than 0.1 a.u. in the DOWS, all the peaks change significantly in both magnitude and location with the surface passivation but in the same manner for all the shells. For instance, for the $[1\bar{1}00]$ field direction, the three peaks in the range 0.3~0.8 a.u. merge into two peaks in the first to third shells when the surface is passivated with the surfactant molecules. The DOWS changes are mainly observed for the local polarizability ranges that are associated with Cd-Se chemical bonds due to the additional local field effect in the presence of trioctylphosphine oxide molecules (Figure 9).

IV. CONCLUSION

In conclusion, the dielectric response of hexagonal cadmium selenide nanowires perpendicular to the wire axis was investigated using first principles quantum mechanical calculations. Scaling behavior of the transverse polarizability was found to closely follow a simple dielectric cylinder model even for the small nanowires with a diameter of a few nanometers. The spatial dependence of the dielectric response in the nanowires was investigated using representation of electronic structure in maximally localized Wannier functions in order to elucidate the simple analytical behavior. Localized d-electrons at cadmium atoms were found responsible for the simple scaling of the polarizability. Our results show that this quantity converges fast with increasing nanowire size and that the core of the nanowire already behaves as bulk CdSe even for a small diameter of ~ 2 nm.

ACKNOWLEDGMENTS

We thank Andra Ferretti (Oxford, UK) for useful discussions and help on Wannier function computation. We acknowledge National Energy Research Scientific Computing Center, which is supported by the Office of Science of the U.S. Department of Energy under Contract No. DE-AC02-05CH11231.

REFERENCE

- ¹ T. A. Pham, T. Li, S. Shankar, F. Gygi, and G. Galli, *Applied Physics Letters* **96** (2010).
- ² A. Singh, X. Li, V. Protasenko, G. Galantai, M. Kuno, H. Xing, and D. Jena, *Nano Letters* **7**, 2999 (2007).
- ³ D. A. Brown, J.-H. Kim, H.-B. Lee, G. Fotouhi, K.-H. Lee, W. K. Liu, and J.-H. Chung, *Sensors* **12**, 5725 (2012).
- ⁴ E. M. Freer, O. Grachev, X. Duan, S. Martin, and D. P. Stumbo, *Nat Nano* **5**, 525 (2010).
- ⁵ B. Kozinsky and N. Marzari, *Physical Review Letters* **96**, 166801 (2006).
- ⁶ G. K. Gueorguiev, J. M. Pacheco, and D. Tománek, *Physical Review Letters* **92**, 215501 (2004).
- ⁷ I. Gur, N. A. Fromer, M. L. Geier, and A. P. Alivisatos, *Science* **310**, 462 (2005).
- ⁸ Y. Yu, P. V. Kamat, and M. Kuno, *Advanced Functional Materials* **20**, 1464 (2010).
- ⁹ Y. Xing, et al., *Nat. Protocols* **2**, 1152 (2007).
- ¹⁰ X. Wu, O. Diéguez, K. M. Rabe, and D. Vanderbilt, *Physical Review Letters* **97**, 107602 (2006).
- ¹¹ N. Marzari and D. Vanderbilt, *Physical Review B* **56**, 12847 (1997).
- ¹² N. Marzari, A. A. Mostofi, J. R. Yates, I. Souza, and D. Vanderbilt, *Reviews of Modern Physics* **84**, 1419 (2012).
- ¹³ G. Paolo, et al., *Journal of Physics: Condensed Matter* **21**, 395502 (2009).
- ¹⁴ J. P. Perdew, K. Burke, and M. Ernzerhof, *Physical Review Letters* **77**, 3865 (1996).
- ¹⁵ D. Vanderbilt, *Physical Review B* **41**, 7892 (1990).
- ¹⁶ I. Souza, J. Íñiguez, and D. Vanderbilt, *Physical Review Letters* **89**, 117602 (2002).
- ¹⁷ A. Calzolari, N. Marzari, I. Souza, and M. Buongiorno Nardelli, *Physical Review B* **69**, 035108 (2004).
- ¹⁸ S. Yang, D. Prendergast, and J. B. Neaton, *Applied Physics Letters* **98** (2011).
- ¹⁹ G. Cicero, A. Ferretti, and A. Catellani, *Physical Review B* **80**, 201304 (2009).
- ²⁰ M. Marcel and T. Christian, *Nanotechnology* **20**, 115707 (2009).
- ²¹ O. Madelung, in *Semiconductors: Data Handbook* (Springer, 2004).

- ²² R. Resta, *Reviews of Modern Physics* **66**, 899 (1994).
- ²³ R. J. Wheatley and T. C. Lillestolen, *Molecular Physics* **106**, 1545 (2008).
- ²⁴ M. Kuno, *Physical Chemistry Chemical Physics* **10**, 620 (2008).
- ²⁵ Y. Yin and A. P. Alivisatos, *Nature* **437**, 664 (2005).
- ²⁶ S. Yang, D. Prendergast, and J. B. Neaton, *Nano Letters* **12**, 383 (2011).

Figures and Tables

	NW-I	NW-II	NW-III	NW-IV
d (Å)	5.5	13.0	20.5	28.0
N	108	432	972	1728
E_{gap} (eV)	2.27	1.75	1.43	1.24
c (Å)	6.91	7.13	7.13	7.13

Table 1. Diameter (d), number of electrons (N), Kohn-Sham energy gap (E_{gap}), and wire axial lattice parameter (c) for the four CdSe nanowires considered in this work (see Figure 1).

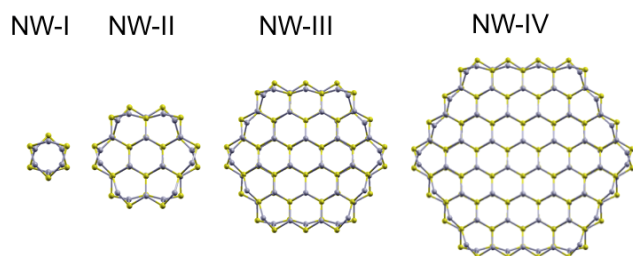


Figure 1. Ball and stick cross-section representation of the four CdSe nanowires with non-polar $(1\bar{1}00)$ lateral surfaces investigated in this work. See Table 1 for the structural details. Yellow (grey) spheres represent selenium (cadmium) atoms.

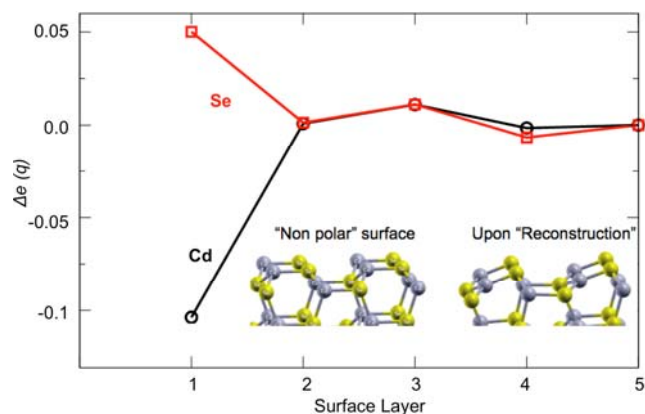


Figure 2. Projected charge differences on cadmium (Cd) and selenium (Se) atoms as a function of the surface layer at the CdSe $(1\bar{1}00)$ face, calculated with respect to the bulk values. Surface relaxation results in significant charge transfer in Cd-Se unit at the top most layer.

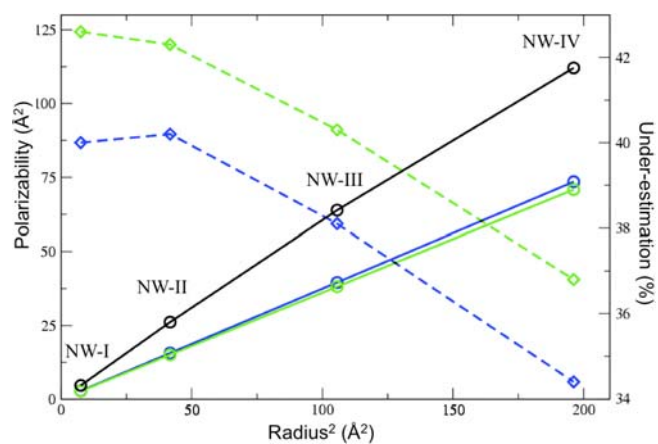


Figure 3. Total transverse polarizability per unit length as a function of the nanowire radius squared (R^2), evaluated from first-principles calculations (black) and by employing a dielectric cylinder model. The latter values were calculated by using either the DFT-PBE bulk dielectric constant (blue) or the experimental one (green). Percentage errors are shown in the right y-axis.

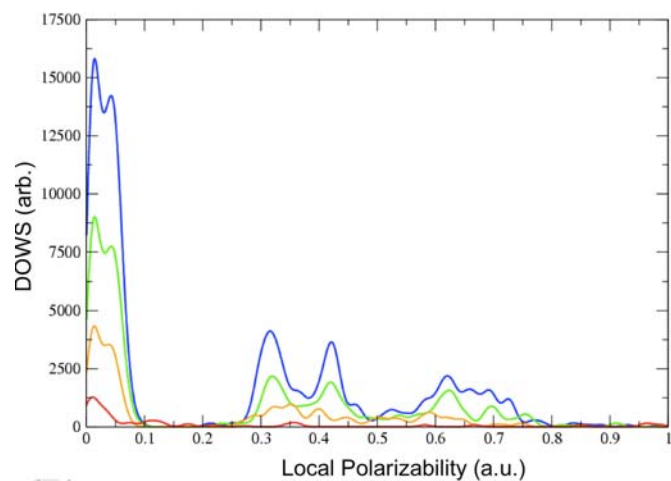


Figure 4. Density of Wannier States (DOWS) as a function of the local polarizability (see text) for NW-I (red), NW-II (orange), NW-III (green), and NW-IV (blue) as in listed in Table 1.

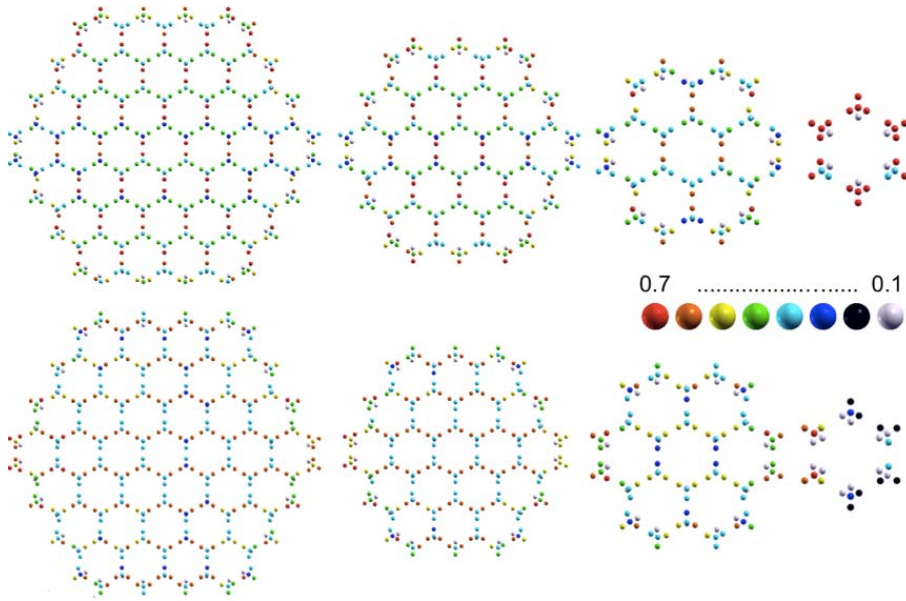


Figure 5. Spatially resolved local polarizability (a.u.) as defined in texts in $[1 \bar{1}00]$ direction (top) and $[11\bar{2}0]$ direction (bottom).

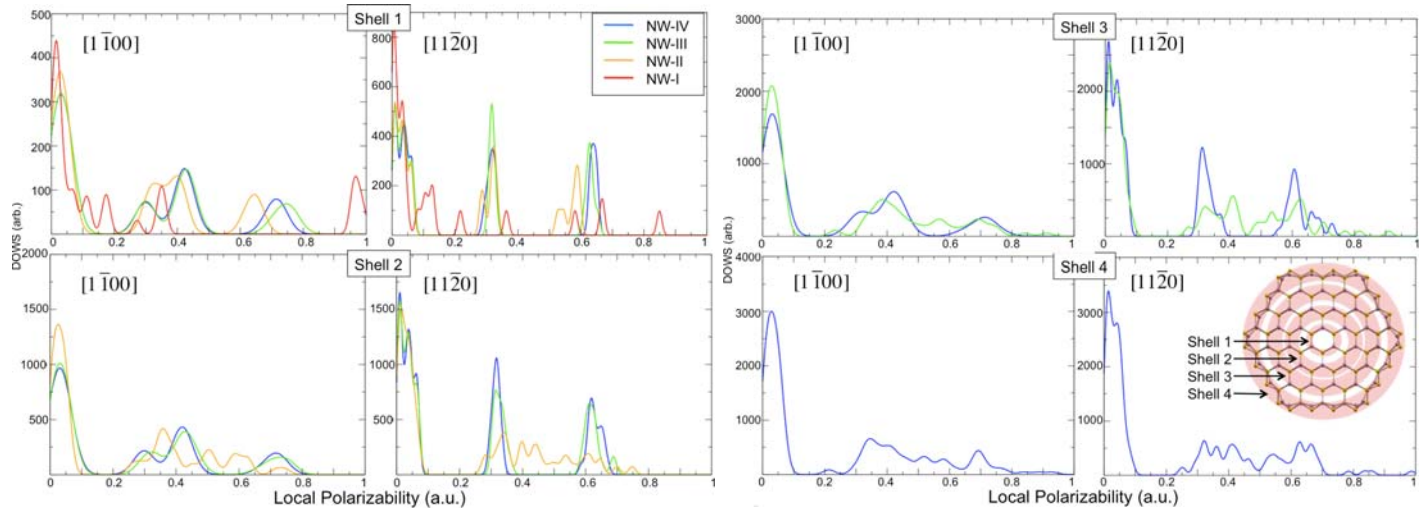


Figure 6. Density of Wannier States (DOWS) as a function of the local polarizability (see text), decomposed in terms of the nanowire concentric shell (see inset), and of the applied electric field direction, for NW-I (red), NW-II (orange), NW-III (green), and NW-IV (blue) as listed in Table 1.

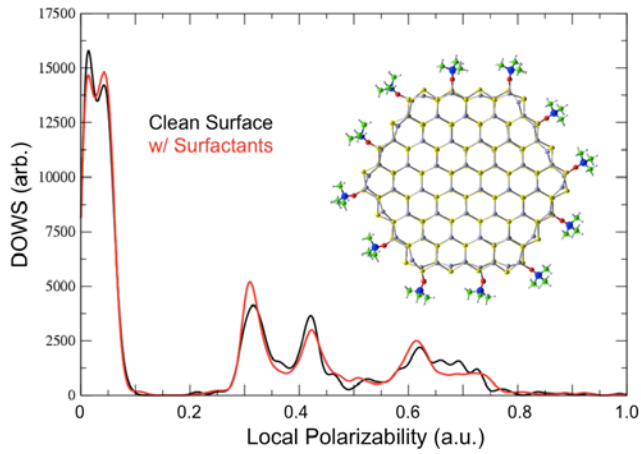


Figure 7. Density of Wannier States (DOWS) as a function of the local polarizability (see text) for NW-IV passivated with trimethylphosphine at 50% coverage.

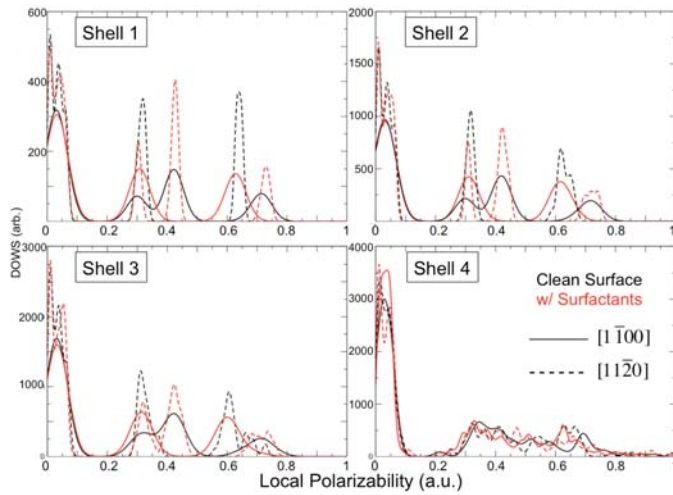


Figure 8. Density of Wannier States (DOWS) as a function of the local polarizability (see text) for NW-IV passivated with trimethylphosphine at 50% coverage, decomposed in terms of the nanowire shell and the electric field direction.

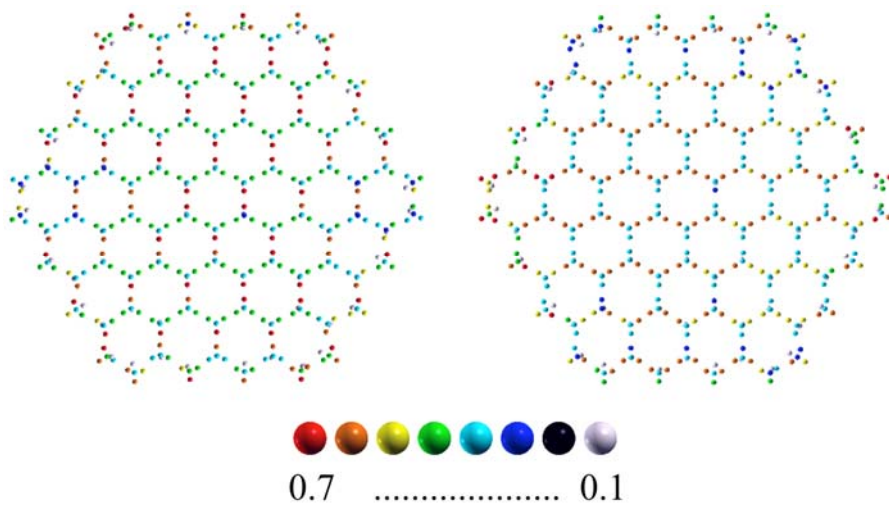


Figure 9. Spatially resolved local polarizability (a.u.) in $[1\bar{1}00]$ direction (left) and $[11\bar{2}0]$ direction (right) for the largest nanowire with the surfactants.